Draft version May 31, 2023
Typeset using LaTeX **twocolumn** style in AASTeX631

The Time-Domain Spectroscopic Survey: Stellar Variability

Benjamin R. Roulston [1], Paul J. Green [2], John J. Ruan [3], Chelsea L. MacLeod, [4] and Scott F. Anderson [5]

[1] *Division of Physics, Mathematics, and Astronomy, California Institute of Technology, Pasadena, CA 91125, USA*
[2] *Center for Astrophysics | Harvard & Smithsonian, 60 Garden St, Cambridge, MA 02138, USA*
[3] *McGill University, 3550 University Street Montreal, QC H3A 2A7, Canada*
[4] *BlackSky, 1505 Westlake Ave N #600, Seattle, WA 98109, USA*
[5] *Department of Astronomy, University of Washington, Box 351580, Seattle, WA 98195, USA*

(Received May 31, 2023)

Submitted to ApJ

ABSTRACT

We present the final variable star sample of the Time-Domain Spectroscopic Survey (TDSS). The TDSS is a Sloan Digital Sky Survey (SDSS)-IV Extended Baryon Oscillation Spectroscopic Survey (eBOSS) subproject that aims to provide classification optical spectra for photometrically variable objects, selected as variable from a combination of SDSS and PanSTARRS light curves only, without other selection criteria. We focus here on the stellar sample of TDSS and report on the 23,595 stars that have TDSS optical spectra and photometric light curves from either the Catalina Sky Survey (CSS) or the Zwicky Transient Facility (ZTF). The variable stars here cover a wide range of spectral types, including both extrinsic and intrinsic variables. We search all light curves for periodic signals and classify the *** systems found to be periodic variables. We provide variability statistics for *** non-periodic objects. We use optical spectra to gain information about the source such as Hα emission, $T_{Eff.}$, and - by incorporating information from Gaia EDR3 - absolute magnitudes and UVW space motions. Using the spectral information in addition to the light curve statistics we build a random forest classifier that can detect and classify variable stars with the additional insights gained from using optical spectra. We find this classifier to have an average of XX% accuracy of distinguishing between different periodic types and an average of XX% accuracy for non-periodic objects. With upcoming large all-sky surveys like LSST, accurate and fast classification will be necessary to work through the upcoming torrent of data, and spectroscopic surveys will be a valuable tool to aid in this classification of variable stars.

Keywords: Variable stars (1761), Surveys (1671), Classification (1907), Time domain astronomy (2109), Light curve classification (1954), Period search (1955), Spectroscopy (1558)

1. INTRODUCTION

Variable stars represent an important tool set in astronomy. They span the entire range of spectral types, temperatures, masses, and stages of stellar evolution. Observations of variable stars can span from photometric, to spectroscopic, to even interferometry. Each of these different technique probe different areas of the variability tree and allow for the determination of different properties of the variability and source. It is no surprise then that many research efforts have been conducted to understand stellar variability. This has mainly focused on many large, all-sky, photometric surveys such as CRTS, ZTF and in the future LSST. However, to date there has not been an effort to undertake a large scale spectroscopic survey of variable stars....more about variables here etc

Corresponding author: Benjamin Roulston
roulston@caltech.edu

2. TDSS VARIABLE STAR PROGRAM

The Time-Domain Spectroscopic Survey (TDSS; Morganson et al. 2015) is an innovative spectroscopic survey aimed at providing an unbiased spectroscopic view of all variables. TDSS is a subprogram of the Sloan Digital Sky Survey IV's (SDSS-IV; Blanton et al. 2017) extended Baryon Acoustic Oscillation Sky Survey (eBOSS; Dawson et al. 2016) project. TDSS was

designed to observe more than 220,000 optical spectra to perform initial characterization and identification of photometrically-variable point sources. The TDSS sample was selected and targeted based on variability between single-epoch SDSS photometry and multi-epoch Pan-STARRS1 3π survey (PS1; Kaiser et al. 2002, 2010) photometry.

The initial TDSS target list was comprised of 135,000 quasars and 85,000 stellar variables (Morganson et al. 2015). These were selected so as to avoid any bias in selection outside of detected variability in the SDSS-PS1 data set (e.g., avoids just reproducing quasar color-cuts from SDSS). This allows TDSS to span more types of variable objects. For example, the TDSS stellar sample is comprised of pulsating variables, eclipsing binaries, cataclysmic variables, chromospherically active stars, as well as other types of stellar variables.

This paper details the stellar variable sample within TDSS's main single-epoch-spectroscopy (SES) program (Morganson et al. 2015). The SES program — along with its pilot survey, dubbed SEQUELS within SDSS-III (Ruan et al. 2016) — primarily targets optical point sources (unconfirmed quasars and stars) for the first epoch of spectroscopy based on variability. Additionally, within several "few-epoch spectroscopy" (FES) subprograms, TDSS also acquires repeat spectroscopic observations for subsets of known stars and quasars that are astrophysically interesting. The FES programs are described by MacLeod et al. (2018) and include several classes of quasars and stars re-targeted to study their spectroscopic variability. The FES stellar programs are not focused here, and more information about those programs can be found in MacLeod et al. (2018); Roulston et al. (2019) (**other FES papers**??).

2.1. *Initial Selection from SDSS and PanSTARRS-1*

The TDSS SES sample selection is described in detail by Morganson et al. (2015). We provide a brief summary here for context.

Morganson et al. (2015) selected the initial TDSS SES sample based on a combination of *griz* photometry from SDSS DR9 (Ahn et al. 2012) (single-epoch) and the PS1 3π survey Kaiser et al. (2002, 2010) (multi-epoch). The SDSS photometry was converted into the PS1 system to allow comparisons directly among those epochs. A three-dimensional kernel density estimator (KDE) was trained on a sample of Strip 82 variable and non-variable objects.

This KDE used three principal parameters: (1) the PS1 SDSS median magnitude difference which captures long-timescale (multi-year) variability; (2) PS1 only variance which describes shorter-timescale (days to a year) variability; and (3) median PS1 magnitudes, which captures the need for larger amplitudes for fainter objects to be detected as variable.

The KDE was used to determine the probability that each object is variable, based on the training sample of Stripe 82 data. This was used to select a uniform 10 objects deg^{-2} to match the TDSS fiber allocation in the SDSS-IV.

2.2. *Sub-sample Optical Spectra*

We select stars from the TDSS sample that have been observed as of the DR16 (Ahumada et al. 2020) of the SDSS-IV as this was the end of the eBOSS and therefore also the end of the TDSS. This includes all spectra up to an MJD of 58543 (2019 March 1). All of these stars were targeted by the TDSS program on the criteria of being variable in a combination of SDSS photometric observations and PanSTARRS. While TDSS is a subprogram of eBOSS and therefore a SDSS-IV program, there was a small pilot program included in the SDSS-III. This Sloan Extended QUasar, Emission Line galaxies, and Luminous red galaxies Survey (SEQUELS) was part of the SDSS-III BOSS survey (Dawson et al. 2013) and observed TDSS targets as well (Ruan et al. 2016). Additionally, during the TDSS target selection, some objects had already been observed during previous iterations of the SDSS and consequentially were excluded from targeting for new eBOSS spectra.

Our spectroscopic sample, therefore, covers spectra from SDSS-I – SDSS-IV, and span MJDs from 51779 (2000 August 23) to 58543 (2019 March 1), with 90% having an observation MJD $>$ 56715 (2014 February 27), near the beginning of SDSS-IV. The majority of the variable stars in our sample are from the TDSS SES program, and we do not focus on any repeat FES spectra in this paper. We do however include the FES `HYPSTAR` targets.

Since the spectroscopic observations for this work are from a combination of SDSS-I/SDSS-II and SDSS-IV spectroscopic data they contain spectra taken with both versions of the SDSS spectrograph. SDSS-I/SDSS-II spectra were taken with the legacy SDSS spectrograph. These data have a wavelength range of 3900–9100Å with a resolution of $R \sim 2000$. The pixel size is 69 km s^{-1}. In SDSS-IV, the new eBOSS spectrograph (Smee et al. 2013) has improved qualities compared to the legacy spectrograph. The eBOSS spectrograph covers the 3,600–10,400Å range, has a resolution of $R \sim 2500$, and has a 1.7Å per pixel size.

While the original target list for TDSS had approximately 85,000 variable stars, as of the end of TDSS (MJD 58543, 2019 March 1), there are only 50,585 stars with spectroscopic observations (3,250 from SEQUELS SDSS-III, 47,335 from TDSS in eBOSS SDSS-IV). We removed all FES targets but kept 675 `HYPSTAR` targets.

We also removed any objects with morphological `CLASS=`GALAXY'` (since many were double or fuzzy, and may have unreliable photometric light curves). We then removed any object with `ZWARNING` or `ZWARNING_NOQSO` > 0, cross-matched to SDSS DR12 (Alam et al. 2015) photometry, and removed any duplicates.

Table 1. Light Curve Properties

LC Survey	$N_{\rm stars}$	$< N_{\rm epochs} >$	$\sigma_{\rm N_{epochs}}$	$<$ mag $>$	$< \sigma_{\rm mag} >$
CSS	21834	264	148	19.36	0.27
ZTF g	18718	197	203	20.22	0.15
ZTF r	24313	311	223	19.59	0.11
ZTF i	15619	34	19	18.82	0.08

Note—Statistics of the three light curve surveys in our variable star sample. For each survey we report the number of stars, the mean number of epochs, the standard deviation of the number of epochs, the mean magnitude, and the mean magnitude error. f

We removed any object for which none of g, r, or i mag are brighter than 20.0, leaving 26,346 stars with spectroscopic observations that meet our quality cuts and cross-matches.

We cross-matched this sample to Gaia EDR3 (Gaia Collaboration et al. 2021) and the distance catalog of Bailer-Jones et al. (2021). This resulted in 25,409 stars with Gaia EDR3 data. This is the sample used to search for optical light curves in both the Catalina Sky Survey and the Zwicky Transient Facility to aid in the classification of variability.

2.3. *Zwicky Transient Facility Light Curves*

We also cross-matched our sample to the Zwicky Transient Facility DR5 (ZTF; Bellm et al. 2019; Masci et al. 2019; Graham et al. 2019). We used the same matching criteria as for the CSS light curves, requiring a match to be within $2''$ of our target coordinates and each star having greater than 10 epochs in each of the available ZTF filters.

In the ZTF g filter there are $18,718$ stars ($\sim$75%) from our sample that meet these criteria. These star's light curves have the following statistics: the median number of epochs is 149, mean is 197. 10% have less than 18 epochs, and 10% have greater than 432 epochs.

In the ZTF r filter there are $24,313$ stars ($\sim$97%) from our sample that meet these criteria. These star's light curves have the following statistics: the median number of epochs is 279, mean is 311. 10% have less than 51 epochs, and 10% have greater than 583 epochs.

We also matched to the ZTF i filter, matching to 15619 stars ($\sim$62%). However, these stars have only a mean of 34 epochs. Therefore, we do not include the ZTF i filter in our sample and analysis.

In this sample, there are 18,651 ($\sim$74%) stars that have light curves in both the ZTF g and r filters. A summary of light curve statistics are reported in Table 1 for all ZTF filters.

2.4. *Final Sample*

Our final sample consists of 25,121 stars selected for variability in the TDSS program. Each of these stars has an SDSS optical spectrum, and at least one light curve from either CSS, ZTF g, or ZTF r.

There are 21,093 ($\sim$84%) stars that have a CSS light curve and a light curve in at least one ZTF filter. There are also 16,476 ($\sim$66%) stars that have light curves in all three light curve surveys (i.e. CSS, ZTF g, ZTF r).

We use v2.0 of the `PyHammer` code (Roulston et al. 2020) to provide spectral classification and radial velocities for the entire sample. This typing also provides the ability to detect specific combinations of double-lined spectroscopic binaries (SB2) from our single epoch spectroscopy.

The on-sky positions of the final SES variable star sample are shown in Figure 1. The TDSS footprint follows that of the eBOSS survey, and there are no objects in our sample below a declination of -7°, or above a declination of 60°.

Figure 2 shows a SDSS color-color diagram for our complete sample. The marker color of each star shows the primary spectral type (e.g. A, F, M, etc.) of the object's spectrum as typed by PyHammer. Our sample covers all spectral types, including a few L dwarfs, C stars, and DA white dwarfs. The spectral types can be seen as a sequence in the color-color diagram. The M-dwarfs (yellow) seem to be smeared out in $u-g$ color space, however this is an artifact of the observations. The M-dwarfs are general faint, especially in the u filter resulting in larger uncertainties, causing the smearing seen.

3. LIGHT CURVE ANALYSIS

Before we use the light curves, we ran a cleaning algorithm to ensure every epoch was good and had a corresponding correct error. For every epoch of every CSS light curve, we compare the reported error to this relationship, and if the reported error is below the fit curve we replace the reported error with the expected error at that magnitude.

Inspecting the ZTF light curves in the same way as the CSS light curves we find that the ZTF errors do not show the same underestimation. Therefore we use the reported ZTF errors, but only include epochs for which the ZTF flag `catflags` == 0 (no ZTF flags), ensuring every epoch is of high quality.

We also perform an outlier removal on all the light curves. We do this by calculating the 5 % and 95% magnitude for each light curve. Using these we select the brightest and faintest 5% of each light curve. We calculate the median magnitude and magnitude error for both the brightest and faintest 5%. From these, we remove any outliers that are brighter or fainter than med(mag) $\mp$ 2×med(mag error) respectively. If this selection drops the number of epochs below 10, we remove that light curve from our analysis.

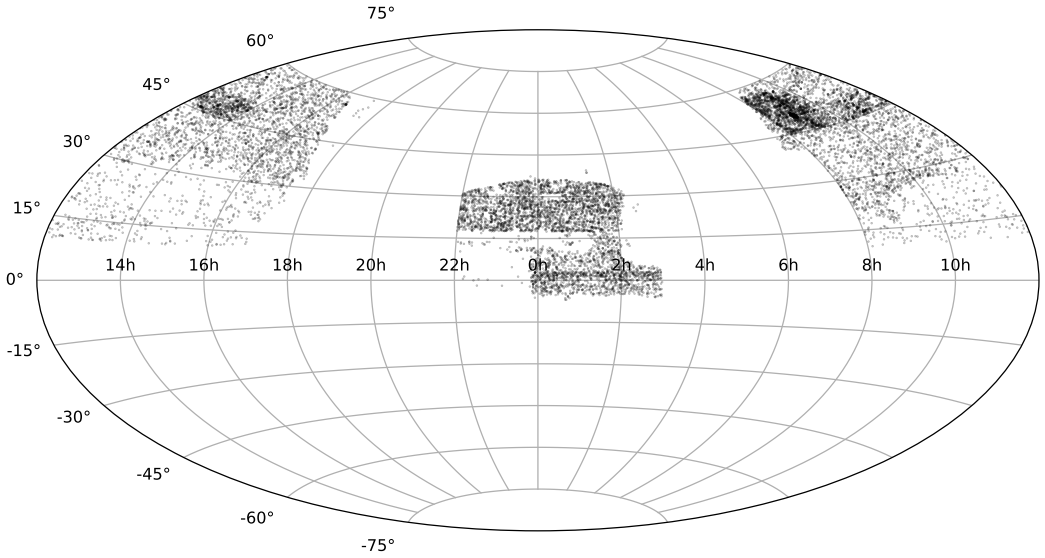

Figure 1. On sky positions and coverage of the TDSS SES sample. This is the final SES variable star sample of 25,121 stars that have an optical SDSS spectrum and at least one light curve. Darker regions represent a higher density of stars. There are no stars in the SES sample below a declination of -7°, or above a declination of 60°.

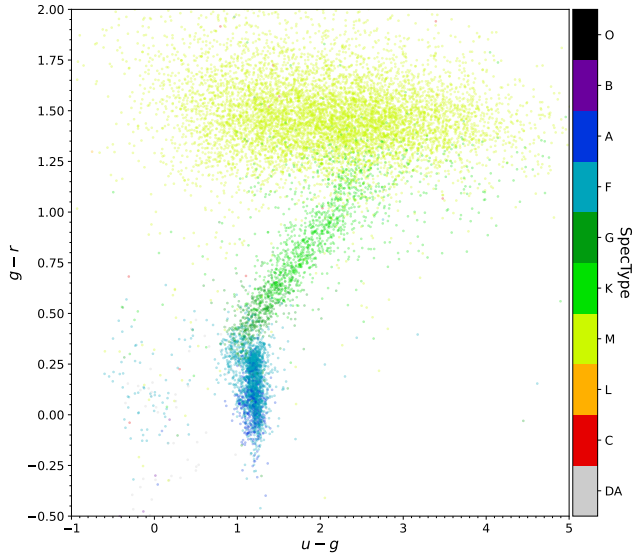

Figure 2. SDSS color-color diagram for our complete SES variable star sample. The marker color for each star is colored according to the primary spectral type as measured by PyHammer. Our sample covers all the primary spectral types and includes a few L-dwarfs, C stars, and DA white dwarfs. The M-dwarfs (yellow) seem to be smeared out in $u-g$ color space, however, this is an artifact of the observations. The M-dwarfs are generally faint, especially in the u filter, resulting in larger uncertainties causing the smearing seen.

We used these filtered light curves to calculate the following statistics.

- N_{epochs}, number of light curve epochs
- $N_{rejects}$, number of epochs rejected from filtering
- μ_{mag}, mean magnitude
- $\mu_{magerror}$, mean magnitude error
- σ_{mag}, light curve standard deviation
- $\tilde{\mu_3}$, light curve skewness
- VarStat $= \sigma_{mag}/\mu_{magerror}$
- a95, 95% amplitude
- $M_t = \frac{\max(mag)-\mathrm{med}(mag)}{\max(mag)-\min(mag)}$, (Kinemuchi et al. 2006)
- conStat, number of sets of 3 consecutive points or more above or below median mag $\pm 2\sigma_{mag}$, (Wozniak 2000; Shin et al. 2009)
- N_{above}, number of epochs above $\mu_{mag} - 2\mu_{magerror}$
- N_{below}, number of epochs below $\mu_{mag} + 2\mu_{magerror}$
- $\chi^2_{const.}$, fit of a constant magnitude model
- χ^2_{linear}, fit of a linear magnitude model
- $\chi^2_{quad.}$, fit of a quadratic magnitude model

Each of these statistics is useful in determining variability, and in the case of periodic variables, can be useful in identifying the type of periodic star.

3.1. *Periodic Variability*

Once the light curve statistics have been calculated, we then search each light curve for periodic signals. We use the Lomb-Scargle periodogram (LS; Lomb 1976; Scargle 1982) to search for periods in our light curves down to a minimum period of 0.1 d. For our LS search, we used the Astropy (Astropy Collaboration et al. 2018) implementation of the LS algorithm (VanderPlas et al. 2012; VanderPlas & Ivezić 2015). We use a set fre-

quency grid for all light curves with 250,000 steps of 0.46296 nHz. This grid provides a fine spacing to ensure all frequencies are searched while reducing the need to compute a frequency grid for every light curve.

For each periodogram

3.2. *Non-periodic Variability*

3.3. *Variability Selection*

The TDSS single epoch spectroscopy sample was targeted using SDSS and PS1 photometry, with details described in Morganson et al. (2015). They report the TDSS sample should be 95% pure in terms of true variable sources. However, not all objects appear to be variable in their ZTF light curves (e.g., they may have $\chi^2 \sim 1$). This is most likely because either the object is truly non-variable, or the magnitude errors are large enough they restrict our ability to detect variability.

To ensure we use the purest variable sample as possible, we make a series of cuts on the light curve features to remove possible non-variables. We first built a control sample by selecting all SDSS objects with spectra with `CLASS=`STAR'` and with `targetType=`STANDARD'`. We crossed matched this sample with ZTF DR6 in the same method as the TDSS sample, and kept only objects with reported ZTF $\chi^2 < 3$. The resulting control sample contains 67,006 objects. We then created a one-to-one match between the TDSS sample and the control sample. We did this by matching each TDSS star to the control star with the closest match in ZTF g and r. The SDSS standard stars on average are brighter than the TDSS sample, and so we also shift the control magnitudes so they match directly the ZTF magnitudes in each filter. We then add noise to the control sample magnitude errors to bring the total error to the expected level for that ZTF magnitude. The result is a control sample of the same size as the TDSS sample with the same magnitude distribution in both ZTf r and g, and with the same g−r color distribution as well. We then calculate the same set of statistics on the control sample as described in Section 3.

Finally, to select our pure variables from the TDSS sample, we use the control sample to make a cut on χ^2, Stetson J, VarStat, Xsigma, and the Lomb-Scargle false-alarm-probability. We require a TDSS star to have any of χ^2, Stetson J, or VarStat greater than the 90% level of the same statistic in the control sample in any filter. Additionally, we count a TDSS star as variable if it has $\log(\mathrm{FAP}) \leq -5$ in any filter, or has a Xsigma statistic from 3.2 that exceeds the 99% level of the control sample in any given bin. This results in a final variable sample of 20169 objects. Figure 4 shows the TDSS sample and control sample distributions for the χ^2, Stetson J, VarStat statistics. The dashed vertical lines represent the 90% level of the control sample which is used to make the cut. The bottom right plot shows the magnitude distributions for the final variable and non-variable samples. The non-variable sample that was removed has fainter magnitudes on average suggesting the larger errors are responsible for the lack of detected variability.

4. SPECTROSCOPIC ANALYSIS

5. MULTI-PARAMETER CLASSIFICATION

5.1. *Principal Identifiable Classes*

5.2. *Unidentifiable Classes*

6. INTERESTING OBJECTS

7. DISCUSSION

Facilities: Sloan

Software: Astropy (Astropy Collaboration et al. 2013, 2018), Corner (Foreman-Mackey 2016), Matplotlib (Hunter 2007), Numpy (Harris et al. 2020), Scipy (Virtanen et al. 2020), Scikit-learn (Pedregosa et al. 2011), TOPCAT (Taylor 2005)

Based on observations obtained with the Samuel Oschin Telescope 48-inch and the 60-inch Telescope at the Palomar Observatory as part of the Zwicky Transient Facility project. ZTF is supported by the National Science Foundation under Grants No. AST-1440341 and AST-2034437 and a collaboration including current partners Caltech, IPAC, the Weizmann Institute for Science, the Oskar Klein Center at Stockholm University, the University of Maryland, Deutsches Elektronen-Synchrotron and Humboldt University, the TANGO Consortium of Taiwan, the University of Wisconsin at Milwaukee, Trinity College Dublin, Lawrence Livermore National Laboratories, IN2P3, University of Warwick, Ruhr University Bochum, Northwestern University and former partners the University of Washington, Los Alamos National Laboratories, and Lawrence Berkeley National Laboratories. Operations are conducted by COO, IPAC, and UW.

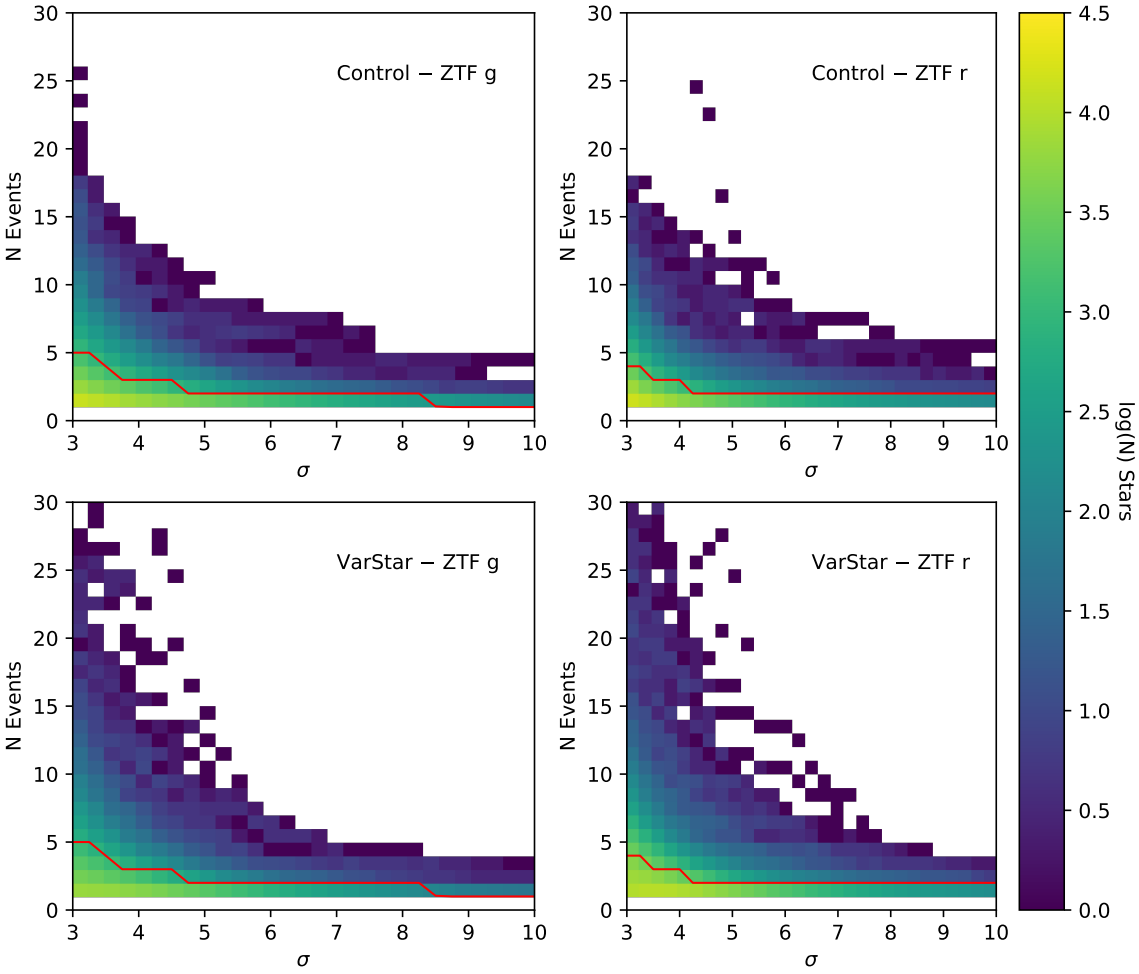

Figure 3. caption

Funding for the Sloan Digital Sky Survey IV has been provided by the Alfred P. Sloan Foundation, the U.S. Department of Energy Office of Science, and the Participating Institutions.

SDSS-IV acknowledges support and resources from the Center for High Performance Computing at the University of Utah. The SDSS website is www.sdss.org.

SDSS-IV is managed by the Astrophysical Research Consortium for the Participating Institutions of the SDSS Collaboration including the Brazilian Participation Group, the Carnegie Institution for Science, Carnegie Mellon University, Center for Astrophysics | Harvard & Smithsonian, the Chilean Participation Group, the French Participation Group, Instituto de Astrofísica de Canarias, The Johns Hopkins University, Kavli Institute for the Physics and Mathematics of the Universe (IPMU) / University of Tokyo, the Korean Participation Group, Lawrence Berkeley National Laboratory, Leibniz Institut für Astrophysik Potsdam (AIP), Max-Planck-Institut für Astronomie (MPIA Heidelberg), Max-Planck-Institut für Astrophysik (MPA Garching), Max-Planck-Institut für Extraterrestrische Physik (MPE), National Astronomical Observatories of China, New Mexico State University, New York University, University of Notre Dame, Observatário Nacional / MCTI, The Ohio State University, Pennsylvania State University, Shanghai Astronomical Observatory, United Kingdom Participation Group, Universidad

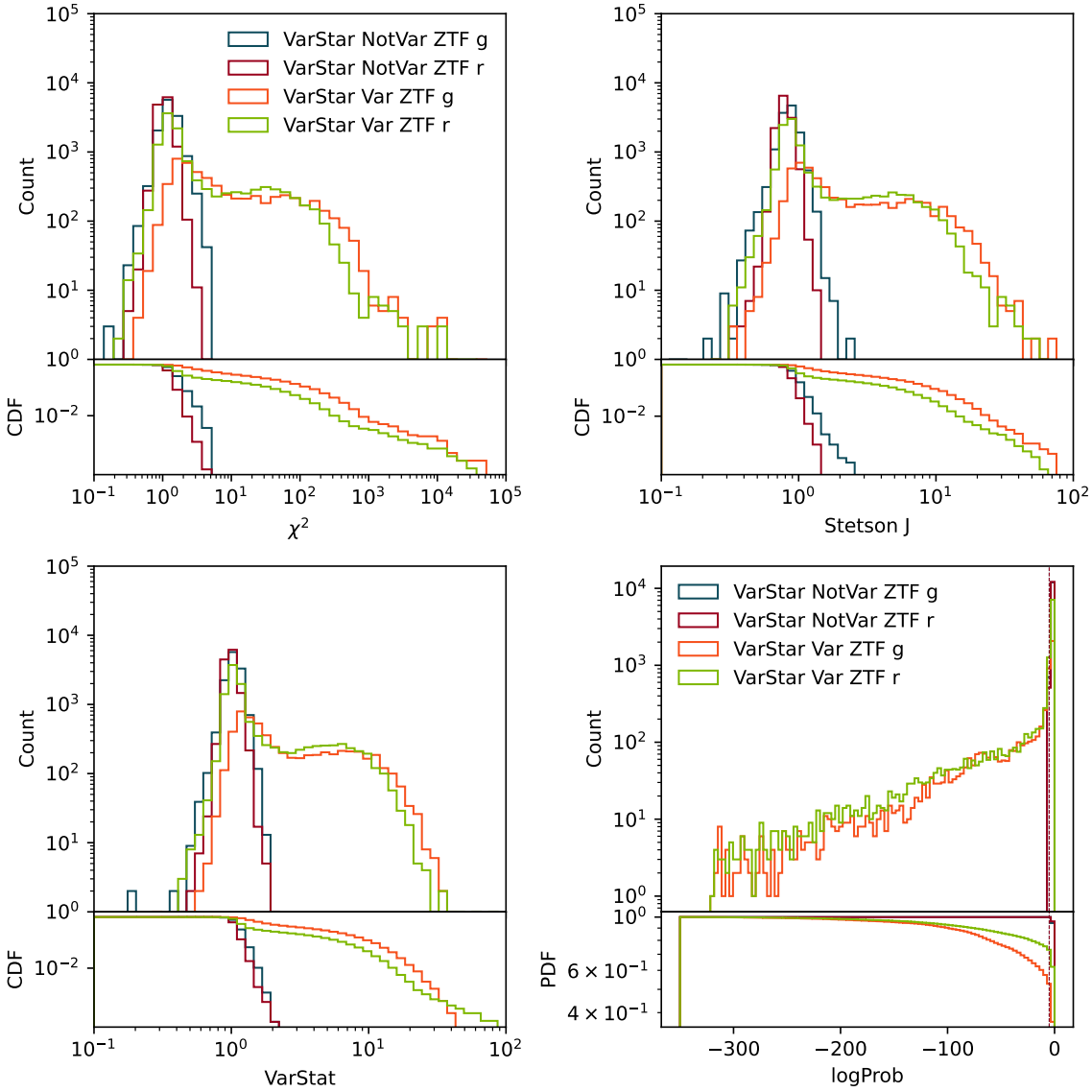

Figure 4. need to add caption here

REFERENCES

Ahn, C. P., Alexandroff, R., Allende Prieto, C., et al. 2012, ApJS, 203, 21, doi: 10.1088/0067-0049/203/2/21

Ahumada, R., Prieto, C. A., Almeida, A., et al. 2020, ApJS, 249, 3, doi: 10.3847/1538-4365/ab929e

Alam, S., Albareti, F. D., Allende Prieto, C., et al. 2015, ApJS, 219, 12, doi: 10.1088/0067-0049/219/1/12

Astropy Collaboration, Robitaille, T. P., Tollerud, E. J., et al. 2013, A&A, 558, A33, doi: 10.1051/0004-6361/201322068

Astropy Collaboration, Price-Whelan, A. M., Sipőcz, B. M., et al. 2018, AJ, 156, 123, doi: 10.3847/1538-3881/aabc4f

Bailer-Jones, C. A. L., Rybizki, J., Fouesneau, M., Demleitner, M., & Andrae, R. 2021, AJ, 161, 147, doi: 10.3847/1538-3881/abd806

Bellm, E. C., Kulkarni, S. R., Graham, M. J., et al. 2019, PASP, 131, 018002, doi: 10.1088/1538-3873/aaecbe

Blanton, M. R., Bershady, M. A., Abolfathi, B., et al. 2017, AJ, 154, 28, doi: 10.3847/1538-3881/aa7567

Dawson, K. S., Schlegel, D. J., Ahn, C. P., et al. 2013, AJ, 145, 10, doi: 10.1088/0004-6256/145/1/10

Dawson, K. S., Kneib, J.-P., Percival, W. J., et al. 2016, AJ, 151, 44, doi: 10.3847/0004-6256/151/2/44

Foreman-Mackey, D. 2016, The Journal of Open Source Software, 1, 24, doi: 10.21105/joss.00024

Gaia Collaboration, Brown, A. G. A., Vallenari, A., et al. 2021, A&A, 649, A1, doi: 10.1051/0004-6361/202039657

Graham, M. J., Kulkarni, S. R., Bellm, E. C., et al. 2019, PASP, 131, 078001, doi: 10.1088/1538-3873/ab006c

Harris, C. R., Millman, K. J., van der Walt, S. J., et al. 2020, Array programming with NumPy, doi: 10.1038/s41586-020-2649-2

Hunter, J. D. 2007, Computing in Science & Engineering, 9, 90, doi: 10.1109/MCSE.2007.55

Kaiser, N., Aussel, H., Burke, B. E., et al. 2002, in Society of Photo-Optical Instrumentation Engineers (SPIE) Conference Series, Vol. 4836, Survey and Other Telescope Technologies and Discoveries, ed. J. A. Tyson & S. Wolff, 154–164, doi: 10.1117/12.457365

Kaiser, N., Burgett, W., Chambers, K., et al. 2010, in Society of Photo-Optical Instrumentation Engineers (SPIE) Conference Series, Vol. 7733, Ground-based and Airborne Telescopes III, ed. L. M. Stepp, R. Gilmozzi, & H. J. Hall, 77330E, doi: 10.1117/12.859188

Kinemuchi, K., Smith, H. A., Woźniak, P. R., McKay, T. A., & ROTSE Collaboration. 2006, AJ, 132, 1202, doi: 10.1086/506198

Lomb, N. R. 1976, Ap&SS, 39, 447, doi: 10.1007/BF00648343

MacLeod, C. L., Green, P. J., Anderson, S. F., et al. 2018, AJ, 155, 6, doi: 10.3847/1538-3881/aa99da

Masci, F. J., Laher, R. R., Rusholme, B., et al. 2019, PASP, 131, 018003, doi: 10.1088/1538-3873/aae8ac

Morganson, E., Green, P. J., Anderson, S. F., et al. 2015, ApJ, 806, 244, doi: 10.1088/0004-637X/806/2/244

Pedregosa, F., Varoquaux, G., Gramfort, A., et al. 2011, Journal of Machine Learning Research, 12, 2825

Roulston, B. R., Green, P. J., & Kesseli, A. Y. 2020, ApJS, 249, 34, doi: 10.3847/1538-4365/aba1e7

Roulston, B. R., Green, P. J., Ruan, J. J., et al. 2019, ApJ, 877, 44, doi: 10.3847/1538-4357/ab1a3e

Ruan, J. J., Anderson, S. F., Green, P. J., et al. 2016, ApJ, 825, 137, doi: 10.3847/0004-637X/825/2/137

Scargle, J. D. 1982, ApJ, 263, 835, doi: 10.1086/160554

Shin, M.-S., Sekora, M., & Byun, Y.-I. 2009, MNRAS, 400, 1897, doi: 10.1111/j.1365-2966.2009.15576.x

Smee, S. A., Gunn, J. E., Uomoto, A., et al. 2013, AJ, 146, 32, doi: 10.1088/0004-6256/146/2/32

Taylor, M. B. 2005, in Astronomical Society of the Pacific Conference Series, Vol. 347, Astronomical Data Analysis Software and Systems XIV, ed. P. Shopbell, M. Britton, & R. Ebert, 29

VanderPlas, J., Connolly, A. J., Ivezic, Z., & Gray, A. 2012, in Proceedings of Conference on Intelligent Data Understanding (CIDU, 47–54, doi: 10.1109/CIDU.2012.6382200

VanderPlas, J. T., & Ivezić, Ž. 2015, ApJ, 812, 18, doi: 10.1088/0004-637X/812/1/18

Virtanen, P., Gommers, R., Oliphant, T. E., et al. 2020, Nature Methods, 17, 261, doi: 10.1038/s41592-019-0686-2

Wozniak, P. R. 2000, AcA, 50, 421. https://arxiv.org/abs/astro-ph/0012143